

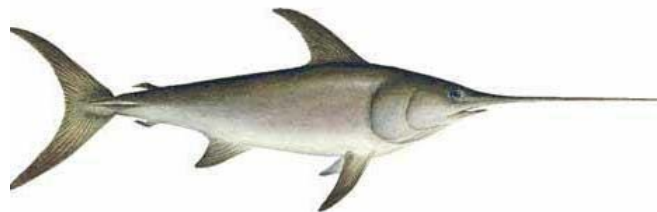
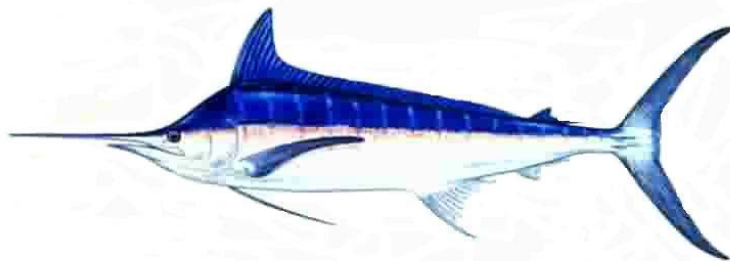


ISC/09/BILLWG-2/02

Development of Bayesian surplus production models for assessing the North Pacific swordfish population

Jon Brodziak
NOAA National Marine Fisheries Service
Pacific Islands Fisheries Science Center
2570 Dole St., Honolulu, Hawaii, 96822 USA

Gakushi Ishimura
Centre for Sustainability Science
Hokkaido University
Kita 9 Nishi 9 Kita-ku, Sapporo, Hokkaido, 060-0809, Japan



**Development of Bayesian surplus production models
for assessing the North Pacific swordfish population**

Jon Brodziak¹ and Gakushi Ishimura²

¹Pacific Islands Fisheries Science Center, Honolulu, HI 96822-2326

²Hokkaido University, Sapporo, Hokkaido 060-0809

Email: Jon.Brodziak@NOAA.GOV and gakugaku@aol.com

ABSTRACT

Bayesian surplus production models were developed for assessing the North Pacific swordfish population. Biomass production was allowed to vary from the symmetric Schaefer curve using an estimated shape parameter. Production models were developed for two stock scenarios: a single-stock scenario and a two-stock scenario with subareas 1 and 2. Input data included nominal landings of North Pacific swordfish during 1951-2006. Relative abundance indices for swordfish consisted of standardized catch-per-unit effort (CPUE) for Japanese, Taiwanese, and U.S. longline fisheries and the California gillnet fishery by stock area. Annual coefficients of variation for CPUE were used to weight the annual uncertainty within each time series of relative abundance indices. Lognormal prior distributions for intrinsic growth rate (r) and carrying capacity (K) were assumed to be moderately precise with coefficients of variation set at 50%. Goodness-of-fit diagnostics were developed for comparing alternative model configurations including the root-mean squared error of CPUE fits and standardized CPUE residuals. Preliminary model fits for 1952-2006 indicated that the Japanese longline CPUE was influential under each scenario because this was the longest time series of relative abundance indices. Preliminary model results also indicated that assumptions about the prior means for intrinsic growth rate and carrying capacity may also be potentially important depending on the model configuration. Overall, the goal of developing operational Bayesian surplus that could incorporate multiple abundance indices and heterogeneous observation errors was achieved. Further work will include refinement of prior assumptions and the capacity to make stochastic catch projections for harvest scenario analyses.

INTRODUCTION

This working paper describes the development of a Bayesian statistical framework to estimate parameters of surplus production models to assess the North Pacific swordfish population. The Bayesian approach provides direct estimates of parameter uncertainty that are easy to interpret and are appropriate for risk analysis. The models include both process error for biomass production dynamics and observation error for the CPUE data from multiple fishing fleets. Production models for alternative stock structure scenarios are formulated; these are a single-stock scenario and a two-stock scenario with subareas 1 and 2. A framework for model averaging to meld results of competing models under a given stock structure scenario is briefly described. Preliminary model results are presented including goodness-of-fit diagnostics along with biomass and harvest rate trends for each stock scenario.

METHODS

Fishery Data

The fishery-dependent catch data for assessing North Pacific swordfish were taken from the most recent summary of data (Courtney and Wagatsuma 2009). Commercial catch biomass data were available for 1952-2006 for each stock scenario.

Estimates of standardized commercial fishery CPUE were also collected from Courtney and Wagatsuma (2009) for each stock scenario. The standardized CPUE time series for the single-stock scenario included Japanese longline CPUE (1952-2006, $n=55$), Taiwanese longline CPUE (1995-2006, $n=12$), Hawaii shallow-set and deep-set longline CPUE (1995-2006, $n=12$), and California gillnet CPUE (1990-2002 and 2005-2006, $n=15$). Under the two-stock scenario, the standardized CPUE time series for subarea 1 included Japanese longline CPUE (1952-2006, $n=55$), Taiwanese longline CPUE (1995-2006, $n=12$), Hawaii shallow-set and deep-set longline CPUE (1995-2006, $n=12$), and California gillnet CPUE (1990-2002 and 2005-2006, $n=15$). Similarly, under the two-stock scenario, the standardized CPUE time series for subarea 2 included Japanese longline CPUE (1955-2006, $n=52$) and Taiwanese longline CPUE (1995-2006, $n=12$).

Production Model

The alternative swordfish production models are formulated as Bayesian-state space models with explicit process and observation error terms (see, for example, Meyer and Millar, 1999). In this case, the unobserved biomass states are estimated from the observed relative abundance indices (CPUE) and catches based on an observation error likelihood function and prior distributions for model parameters (θ). The observation error likelihood measures the discrepancy between observed and predicted CPUE.

The process dynamics are based on a power function surplus production model with an annual time step. Under this 3-parameter model, current biomass (B_T) depends on the previous biomass, catch (C_{T-1}), the intrinsic growth rate (R), carrying capacity (K), and a production shape parameter (M) for $T = 2, \dots, N$.

$$(1) \quad B_T = B_{T-1} + R \cdot B_{T-1} \left(1 - \left(\frac{B_{T-1}}{K} \right)^M \right) - C_{T-1}$$

The shape parameter $M > 0$ determines where surplus production peaks as biomass varies in proportion to carrying capacity. If $0 < M < 1$, surplus production peaks when biomass is below $\frac{1}{2}$ of K (i.e., a right-skew production curve). If $M > 1$, then biomass production is higher when biomass is above $\frac{1}{2}$ of K (i.e., a left-skewed production curve). If $M = 1$, the production model is identical to a discrete-time version of the Schaefer production model where maximum surplus production occurs when biomass is equal to $\frac{1}{2}$ of K . The values of biomass and harvest rate that maximize surplus production are relevant as biological reference points. For the discrete-time power function model, the biomass that maximizes surplus production (B_{MSY}) is

$$(2) \quad B_{MSY} = K \cdot (M + 1)^{-\frac{1}{M}}$$

The corresponding harvest rate that maximizes surplus production (H_{MSY}) is

$$(3) \quad H_{MSY} = R \left(1 - \frac{1}{M + 1} \right)$$

and the maximum surplus production (MSY) is

$$(4) \quad MSY = R \left(1 - \frac{1}{M + 1} \right) \cdot K (M + 1)^{-\frac{1}{M}}$$

The power function model can be reparameterized in terms of the proportion of carrying capacity ($P = B/K$) to improve the efficiency of the Markov Chain Monte Carlo algorithm used to estimate parameters. Based on this parameterization, the process dynamics for the power function model are

$$(5) \quad P_T = P_{T-1} + R \cdot P_{T-1} \left(1 - P_{T-1}^M \right) - \frac{C_{T-1}}{K}$$

The process dynamics are subject to natural variation as a result of fluctuations in life history parameters, trophic interactions, environmental conditions and other factors. In this context, the process error represents the joint effect of a large number of random multiplicative events which combine to form a multiplicative lognormal process under the Central Limit Theorem. In particular, the process error terms are assumed to be independent and lognormally distributed random variables $\eta_T = e^{U_T}$ where the U_T are normal random variables with mean 0 and variance σ^2 .

The state equations define the stochastic process dynamics by relating the unobserved biomass states to the observed catches and the population dynamics parameters. Given

the lognormal process error assumption, the state equations for the initial time period $T = 1$ and subsequent periods $T > 1$ are

$$(6) \quad \begin{aligned} P_1 &= \eta_1 \\ P_T &= \left(P_{T-1} + R \cdot P_{T-1} (1 - P_{T-1}^M) - \frac{C_{T-1}}{K} \right) \cdot \eta_T \end{aligned}$$

These equations set the conditional prior distribution for the proportion of carrying capacity, $p(P_T)$, in each time period T , conditioned on the previous proportion.

Observation Error Model

The observation error model relates the observed fishery CPUE to the exploitable biomass of the swordfish stock under each scenario. It is assumed that each CPUE index (I) is proportional to biomass with catchability coefficient Q

$$(7) \quad I_T = QB_T = QKP_T$$

The observed CPUE dynamics are also subject to natural sampling variation which is assumed to be lognormally distributed. The observation errors are $\nu_T = e^{V_T}$ where the V_T are iid normal random variables with zero mean and weighted variance $(W_T \cdot \tau)^2$ with standard deviation τ and weighting factor W_T . The variance weights W_T reflect the relative uncertainty of the CPUE index value in year T and are scaled using the coefficient of variation (CV) of the difference between the observed and predicted log-transformed biomass indices (Maunder and Starr 2003). These weights were calculated from the relative coefficients of variation of each annual CPUE index as $W_T = CV[CPUE_T] / \min(CV[CPUE])$.

Given the lognormal observation errors, the observation equations for $T = 1, \dots, N$ are

$$(8) \quad I_T = QKP_T \cdot \nu_T$$

This specifies the observation error likelihood function $p(I_T|\theta)$ for each period.

Prior Distributions

Under the Bayesian paradigm, prior distributions are employed to quantify existing knowledge (or the lack thereof) of the likely value of each model parameter. In this context, the model parameters consist of the carrying capacity, intrinsic growth rate, shape parameter, catchability, the process and observation error variances, and the initial biomass as a proportion of carrying capacity. Unobserved biomass states are the proportions of carrying capacity, P_T , for $T > 1$, conditioned on the previous proportion. In general, auxiliary information was incorporated into the prior distributions when it was available.

Prior for Carrying Capacity

The prior distribution for the carrying capacity $p(K)$ was chosen to be a lognormal distribution with mean (μ_K) and variance (σ_K^2) parameters set to achieve a CV of 50%

$$(9) \quad p(K) = \frac{1}{\sqrt{2\pi}\sigma_K} \exp\left(-\frac{(K - \mu_K)^2}{2\sigma_K^2}\right)$$

The mean K parameter was set to be 150 kt under the single stock scenario. For the two-stock scenario, the mean K for subarea 1 was set to be 150 kt while the mean K for subarea 2 was set to be 75 kt. These mean values were chosen to reflect the biomass likely needed to support the observed fishery catches in each scenario. The sensitivity of production model results to uncertainty in the prior mean of K was further investigated in Ishimura and Brodziak (2009).

Prior for Intrinsic Growth Rate

The prior distribution for intrinsic growth rate $p(R)$ was chosen to be a lognormal distribution with mean (μ_R) and variance (σ_R^2) parameters set to achieve a CV of 50%

$$(10) \quad p(R) = \frac{1}{\sqrt{2\pi}\sigma_R} \exp\left(-\frac{(R - \mu_R)^2}{2\sigma_R^2}\right)$$

The mean R parameter was set to be $\mu_R=0.5$ for each stock scenario. This mean value was consistent with the range of prior means of (0.40, 0.43) estimated for North and South Atlantic swordfish, respectively, using demographic data (McAllister et al. 2000). A similar analysis for North Pacific swordfish using the mean generation time approach (e.g., McAllister et al. 2001) suggested that higher values of $R \approx 0.9$ to 1.0 may be appropriate; this analysis assumed female growth and maturation from DeMartini et al. (2000) and DeMartini et al. (2007) and five alternative natural mortality rate estimators (Hoenig, Alverson and Carney, Pauly, Beverton-Holt 2nd invariant, and Lorenzen Tropical) from Brodziak (2009) to calculate five alternative estimates of R. In this case, the primary difference between the Atlantic and Pacific swordfish demographic data were the values of natural mortality. McAllister et al. (2000) assumed a constant natural mortality rate of $M=0.2$ while the Pacific swordfish natural mortality was based on an average of five estimators from Brodziak (2009) with a central tendency of $M \approx 0.35$. Setting the prior mean of $R = 0.5$ with a CV of 50% allowed enough flexibility for the production model to discern the more probable range of R given the observed catch and CPUE data. Nonetheless, there was considerable uncertainty in what was deemed an appropriate prior mean for R. As a result, the sensitivity of production model results to uncertainty in the prior mean of K was further investigated in Ishimura and Brodziak (2009).

Prior for Production Shape Parameter

The prior distribution for the production function shape parameter $p(M)$ was chosen to be a gamma distribution with scale parameter λ and shape parameter k :

$$(11) \quad p(M) = \frac{\lambda^k M^{k-1} \exp(-\lambda M)}{\Gamma(k)}$$

The values of the scale and shape parameters were set to $\lambda = k = 2$. This choice set the mean of $p(M)$ to be $\mu_M = 1$, which corresponds to the value of M under the Schaefer production model. This choice also implied that the CV of the shape parameter prior was 71%. In effect, the shape parameter prior was centered on the symmetric Schaefer model as the default with enough flexibility to estimate a nonsymmetric production function if needed.

Prior for Catchability

The prior for catchability $p(Q)$ was chosen to be a diffuse inverse-gamma distribution with scale parameter λ and shape parameter k .

$$(12) \quad p(Q) = \frac{\lambda^k Q^{-(k+1)}}{\Gamma(k)} \exp\left(\frac{-\lambda}{Q}\right)$$

The scale and shape parameters were set to be $\lambda = k = 0.001$. This choice of parameters implies that $1/Q$ has a mean of 1 and a variance of 1000. As a result, the prior for catchability was approximately $p(Q) \propto Q^{-1}$. Since $1/Q$ is unbounded at $Q = 0$, an additional numerical constraint that Q lie within the interval $[0.0001, 10]$ was imposed.

Priors for Error Variances

Priors for the process error variance $p(\sigma^2)$ and observation error variance $p(\tau^2)$ were chosen to be inverse-gamma distributions, a natural choice for dispersion priors (Congdon, 2001). For the process error variance prior, the scale parameter was set to $\lambda = 4$ and the shape parameter was $k = 0.01$. This choice of parameters produces a CV for σ of 16%. Similarly, for the observation error variance prior, the scale parameter was set to $\lambda = 2$ and the shape parameter was $k = 0.01$. This choice of parameters gives a CV of 22% for τ (recall that the annual observation errors include a year-specific weighting factor). Given these prior assumptions, the initial observation error variance was assumed to be roughly 40% greater than the process error variance.

Priors for Proportions of Carrying Capacity

Prior distributions for the time series of biomass in proportion to carrying capacity, $p(P_T)$, are determined by the lognormal distributions specified in the process dynamics. The mean proportion of carrying capacity for the initial time period (1952 for single-stock and 1951 for two-stock scenarios) was set to 0.9 for each region in the absence of information on the likely value.

Posterior Distribution

The joint posterior distribution needs to be calculated to make inferences about the model parameters. From Bayes' theorem, the posterior distribution given catch and CPUE data D , $p(\theta|D)$, was proportional to the product of the priors and the likelihood of the CPUE data.

$$(13) \quad p(\theta|D) \propto p(K)p(R)p(M)p(Q)p(\sigma^2)p(\tau^2)\prod_{T=1}^N p(P_T)\prod_{T=1}^N p(I_T|\theta)$$

There was no closed form expression to calculate parameter estimates from the posterior distribution.

Parameter estimation for multiparameter nonlinear Bayesian models, such as the swordfish production model, is typically based on simulating a large number of independent samples from the posterior distribution. In this case, Markov Chain Monte Carlo (MCMC) simulation (Gilks et al., 1996) was applied to numerically generate a sequence of samples from the posterior distribution. The WINBUGS software (Spiegelhalter et al., 2003) was used to set the initial conditions, perform the MCMC calculations, and summarize the results.

MCMC simulations were conducted in an identical manner for each of the swordfish stock structure scenarios models described below. Three chains of 60,000 samples were simulated in each model run. The first 10,000 samples of each chain were excluded from the estimation process. This burn-in period removed any dependence of the MCMC samples on the initial conditions. Next, each chain was thinned by 2 to remove autocorrelation. That is, every other sample was used for inference. As a result, 75,000 samples from the posterior were used for summarizing model results. Convergence of the MCMC simulations to the posterior distribution was checked using the Brooks-Gelman-Rubin (BGR) convergence diagnostic (Brooks and Gelman, 1998). This diagnostic was monitored for several key model parameters (intrinsic growth rate, carrying capacity, production function shape parameter, catchability coefficients) to verify convergence.

Goodness-of-Fit Criteria

Model residuals were used to measure the goodness of fit of the alternative production models. Residuals for the CPUE series are the log-scale observation errors ε_T .

$$(14) \quad \varepsilon_T = \ln(I_T) - \ln(QKP_T)$$

Non-random patterns in the residuals indicated that the observed CPUE did not conform to one or more model assumptions. The root mean-squared error (RMSE) of the CPUE fit provided another diagnostic of the model goodness of fit with lower RMSE indicating a better fit when comparing models with the same number of parameters.

The Bayesian information criterion (BIC) provided another goodness-of-fit measure for comparing alternative production models applied to the same stock scenario data. In this case, the model with the lowest BIC value provided the best fit to the multifleet CPUE

data. The BIC value for the i^{th} model of a set of N_S alternative models with maximized value L_i for the joint observation error likelihood function, p_i parameters, and n data points was

$$(15) \quad BIC_i = -2 \cdot L_i + p_i \cdot \log(n)$$

The exponential of minus one half times the difference in BIC values between the i^{th} and the best-fitting swordfish production model (S_0) at the k^{th} MCMC iterate ($\Delta_i^{(k)}$) can be used to approximate the Bayes factor ($B_{i,o}^{(k)}$), or the relative odds that model S_i versus S_0 was the true model via

$$(16) \quad B_{i,o}^{(k)} \approx \exp\left(-\frac{1}{2}(BIC_i^{(k)} - BIC_0^{(k)})\right) = -\frac{1}{2}\Delta_i^{(k)}$$

If each alternative model was assigned an equal prior weight of $\Pr(M_i) = 1/N_S$ and was fit to the same stock scenario data D_j , then the posterior probability that swordfish model S_i was the true model under stock structure scenario j ($\Pr(S_i | D_j)$) could be calculated from the 75,000 MCMC samples as

$$(17) \quad \Pr(S_i | D_j) = \frac{\Pr(S_i) \cdot B_{i,0}}{\sum_m \Pr(S_m) \cdot B_{m,0}} \approx \frac{1}{75000} \sum_{k=1}^{75000} \frac{\exp(-0.5\Delta_i^{(k)})}{\sum_m \exp(-0.5\Delta_m^{(k)})}$$

This approach to model comparison and averaging was applied to account for uncertainty in prior means of swordfish intrinsic growth rate and carrying capacity parameters by Ishimura and Brodziak (2009).

RESULTS

Convergence to Posterior Distribution

The BGR diagnostic was monitored for the intrinsic growth rate, carrying capacity, production function shape parameter, and catchability coefficients under both stock structure scenarios. In all cases, the BGR values were approximately unity which was consistent with the convergence in distribution of the MCMC samples to the posterior distribution.

Density plots of the posterior distributions of the intrinsic growth rate, carrying capacity, production function shape parameter, and catchability coefficients were smooth and unimodal under both stock structure scenarios. This empirical check was also consistent with a convergent sequence of MCMC samples. Overall, it appeared that the MCMC samples generated from the Bayesian production model numerically converged to the posterior distribution.

Single-Stock Scenario Model Fits to CPUE

Results of the fits to standardized CPUE under the single-stock scenario indicated that the Japanese longline CPUE had the lowest RMSE while the California Gillnet CPUE had the poorest fit (Table 1). Predicted Japanese CPUE appeared to randomly fluctuate about the observed CPUE time series (Figure 1.1). Examination of the log-scale residuals indicated that there was a significant increasing trend with time ($P < 0.02$) and that the residuals were normally distributed ($P < 0.87$). The fit to the observed Taiwanese longline CPUE had a pattern of consecutive negative residuals that appeared non-random (Figure 1.2). However, there was no trend in residuals ($P < 0.07$) and the log-scale residuals were normally distributed ($P < 0.17$). Similarly, the fits to the Hawaii shallow-set longline CPUE had a negative then positive pattern of residuals (Figure 1.3) but no trends in residuals were detected during 1995-2000 ($P < 0.12$) or during 2004-2006 ($P < 0.16$). In both periods, the log-scale residuals were normally distributed ($P < 0.53$). For the Hawaii deep-set longline CPUE there was a pattern of negative residuals during 1999-2006 (Figure 1.4). However, there was no detectable trend in residuals ($P < 0.26$) and the log-scale residuals were normally distributed ($P < 0.83$). The fit to the California gillnet CPUE (Figure 1.5) had no trend in residuals ($P < 0.95$) and had log-scale residuals that were normally distributed ($P < 0.08$). Overall, under the single-stock scenario, the fits to the CPUE time series exhibited some non-random patterns and lack of conformance to model error assumptions.

Two-Stock Scenario Model Fits to CPUE

Under the two-stock scenario, results of the fits to standardized CPUE indicated that the Japanese longline CPUE had the lowest RMSE while the California Gillnet CPUE had the highest RMSE (Table 1). Predicted Japanese CPUE fluctuated around the observed CPUE time series (Figure 2.1). The log-scale residuals had no time trend ($P < 0.16$) and were normally distributed ($P < 0.55$). The Taiwanese longline CPUE fit had a pattern of consecutive negative residuals in the late-1990s (Figure 2.2). There was a detectable time trend in the residuals ($P < 0.03$) and the log-scale residuals were normally distributed ($P < 0.29$). Fits to the Hawaii shallow-set longline CPUE appeared to have an increasing trend in residuals (Figure 2.3). There was a significant increasing trend during 1995-2000 ($P < 0.02$) but no detectable trend during 2004-2006 ($P < 0.10$). The log-scale residuals were normally distributed in both periods ($P < 0.38$ and $P < 0.70$). The fit to the Hawaii deep-set longline CPUE had no clear pattern in residuals during 1999-2006 (Figure 2.4) and there was no detectable trend in residuals ($P < 0.45$). The log-scale residuals for this fit were also normally distributed ($P < 0.14$). Similarly, the fit to the California gillnet CPUE (Figure 2.5) had no apparent trend in residuals ($P < 0.46$) and the log-scale residuals were normally distributed ($P < 0.64$). Overall, some of the fits to the CPUE time series in subarea 1 under the two-stock scenario exhibited non-random patterns and the Taiwanese and Hawaii shallow-set long CPUE fits had increasing trends in their residual patterns.

For subarea 2 under the two-stock scenario, the model fits to standardized CPUE indicated that the Japanese longline CPUE had a lower RMSE than the fit to the Taiwanese CPUE (Table 1). The fit to the Japanese longline CPUE (Figure 3.1) exhibited some large negative residuals in the 1950s but otherwise appeared to fluctuate randomly about the observed CPUE. The residuals had a significant increasing trend ($P < 0.01$) and

the log-scale residuals were not normally distributed ($P < 0.01$). In contrast, there was no apparent pattern in the fit to the Taiwanese longline CPUE (Figure 3.2). In this case, the residuals had no detectable trend ($P < 0.58$) and the log-scale residuals were normally distributed ($P < 0.32$). Overall, in subarea 2 there was a good fit to the Taiwanese longline CPUE and a lack of fit to the Japanese longline in the 1950s.

Model Parameters and Reference Points

Estimates of production model parameters varied between the stock structure scenarios (Table 2). Under the single-stock scenario, the intrinsic growth rate was estimated to be $R = 0.76$. In contrast, under the two-stock scenario the estimates of R were 0.63 and 0.41 for subareas 1 and 2, or 17% and 46% below the single-stock estimate. The estimate of K under the single-stock scenario ($K = 88.3$ kt) was about 42% less than the sum of the estimates of K under the two-stock scenario ($K_1 + K_2 = 150.0$ kt). The estimate of the production model shape parameter for the single-stock scenario was $M = 1.27$ indicating a left-skewed production curve. In comparison the estimate of M_1 for subarea 1 was approximately 1 indicating a symmetric biomass production curve while the M_2 estimate for subarea 2 was $M_2 = 0.59$ indicating a right-skewed production curve. Overall, estimates of production model parameters R , K , and M differed between the stock scenarios.

Estimates of biological reference points also differed between the stock scenarios (Table 2). The mean estimate of B_{MSY} under the single-stock scenario was $B_{MSY} = 45.7$. This was about 38% below the sum of the estimates of B_{MSY} under the two-stock scenario. The mean estimate of H_{MSY} under the single-stock scenario was $H_{MSY} = 0.39$. In comparison, the estimates of H_{MSY} under the two-stock scenario were 0.29 and 0.13 for subareas 1 and 2, or 26% and 67% less than the single-stock estimate. In contrast, the mean estimate of MSY under the single-stock scenario was $MSY = 17.2$ kt which was only 3% higher than the sum of the MSY estimates under the two-stock scenario. Overall, the results indicated that the North Pacific swordfish population would be considered to be a smaller and more productive under the single-stock scenario than under the two-stock scenario.

In contrast to the estimates of production model parameters and biological reference points, there was no practical difference in the estimates of stock status in 2006 between the two stock scenarios (Table 2). In particular, the mean estimates of B_{2006} were greater than B_{MSY} under both stock scenarios and subareas and the associated probabilities of B_{2006} exceeding B_{MSY} were 1 except for subarea 1 where that probability was 0.82. Similarly, mean estimates of exploitation rate in 2006 were below H_{MSY} for both stock scenarios and subareas and the corresponding probabilities that H_{2006} exceeded H_{MSY} were no greater than 0.01. This indicated that the choice of stock scenario had no practical impact on the status of the North Pacific swordfish population with respect to MSY -based reference points.

Estimates of Exploitable Biomass and Exploitation Rate

Under the single-stock scenario, exploitable biomass fluctuated about B_{MSY} during the 1950s to 1980s (Figure 4.1). Biomass then increased above B_{MSY} in the late-1980s, subsequently declined to below B_{MSY} in the late-1990s, and increased to above B_{MSY} in

the 2000s. Exploitation rates were below H_{MSY} in the early-1950s, increased to a peak of about 45% around 1960, and subsequently declined to less than H_{MSY} during 1965-1990 (Figure 4.1). Exploitation rates increased in the early-1990s to fluctuate around H_{MSY} and subsequently declined in the early-2000s to roughly $\frac{1}{2}$ of H_{MSY} . Under the single-stock scenario, exploitable biomass generally remained above B_{MSY} and exploitation rates remained below H_{MSY} throughout the assessment time horizon.

Exploitable biomass of the swordfish stock in subarea 1 under the two-stock scenario also fluctuated around B_{MSY} for most of the assessment time horizon (Figure 4.2). Biomass increased to above B_{MSY} during 1985-1995 and has since declined to roughly B_{MSY} . Exploitation rates in subarea 1 increased from low values in the 1950s to a peak of about 40% around 1960 and then declined to fluctuate about $\frac{1}{2}$ of H_{MSY} from the mid-1960s to the late-1980s. Exploitation rates increased to fluctuate about H_{MSY} during the 1990s and then declined in the 2000s to about $\frac{2}{3}$ of H_{MSY} . Overall, exploitable biomass in subarea 1 remained at or above B_{MSY} while exploitation rates remained at or below H_{MSY} throughout the assessment time horizon.

Exploitable biomass in subarea 2 under the two-stock scenario was at or above B_{MSY} throughout the assessment time horizon (Figure 4.3). Biomass increased to a peak around 2000 and has since declined in the 2000s, albeit to a level well-above B_{MSY} . Exploitation rates in subarea 2 remained at or below H_{MSY} throughout the assessment time horizon (Figure 4.3). Overall, the stock in subarea 2 has not been depleted or experienced overfishing under this model scenario.

ACKNOWLEDGMENTS

We thank Lyn Wagatsuma and Eric Fletcher for their help in preparing this document.

REFERENCES

- Brodziak, J. 2009. Potential natural mortality rates of North Pacific swordfish. International Scientific Committee for Tuna and Tuna-Like Species in the North Pacific/Billfish WG, ISC/09/BILLWG-1/13, 20 p.
- Brooks, S. P., and A. Gelman. 1998. Alternative methods for monitoring convergence of iterative simulations. *Journal of Computational and Graphical Statistics*, 7:434–455.
- Congdon, P. 2001. Bayesian statistical modeling. Wiley, New York, 531 p.
- Courtney, D., and L. Wagatsuma. 2009. Input data for a North Pacific swordfish stock assessment using Bayesian production models. International Scientific Committee for Tuna and Tuna-Like Species in the North Pacific/Billfish WG, ISC/09/BILLWG-2/01.
- DeMartini, E., J. Uchiyama, H. Williams. 2000. Sexual maturity, sex ratio, and size composition of swordfish, *Xiphias gladius*, caught by the Hawaii-based pelagic longline fishery. *Fish. Bull.* 98:489-506.

DeMartini, E., J. Uchiyama, R. Humphreys, Jr., J. Sampaga, and H. Williams. 2007. Age and growth of swordfish (*Xiphias gladius*) caught by the Hawaii-based pelagic longline fishery. *Fish. Bull.* 105:356-367.

Gilks, W. R., S. Richardson, and D. J. Spiegelhalter. [Eds.] 1996. *Markov Chain Monte Carlo in Practice*. Chapman and Hall, London. 486 p.

Ishimura, G. and J. Brodziak. 2009. Model-averaging to account for prior uncertainty in swordfish intrinsic growth rate and carrying capacity. International Scientific Committee for Tuna and Tuna-Like Species in the North Pacific/Billfish WG, ISC/09/BILLWG-2/03.

Maunder, M. and P. Starr. 2003. Fitting fisheries models to standardized CPUE abundance indices. *Fish. Res.* 63:43-50.

McAllister, M., E. Babcock, E. Pikitch, and M. Prager. 2000. Application of a non-equilibrium generalized production model to South and North Atlantic swordfish: Combining Bayesian and demographic methods for parameter estimation. *Col. Vol. Sci. Pap. ICCAT*, 51(5):1523-1550.

McAllister, M., E. Pikitch, and E. Babcock. 2001. Using demographic methods to construct Bayesian priors for the intrinsic rate of increase in the Schaefer model and implications for stock rebuilding. *Can. J. Fish. Aquat. Sci.* 58:1871-1890.

Meyer, R., and R. Millar. 1999. BUGS in Bayesian stock assessments. *Can. J. Fish. Aquat. Sci.* 56:1078-1086.

Spiegelhalter, D., A. Thomas, N. Best, and D. Lunn. 2003. *WinBUGS User Manual*. Available at: <http://www.mrc.bsu.carn.ac.uk/bugs/winbugs/manual14.pdf>

Table 1. Root mean-squared errors of model fits to CPUE time series under the single-stock and two-stock scenarios.

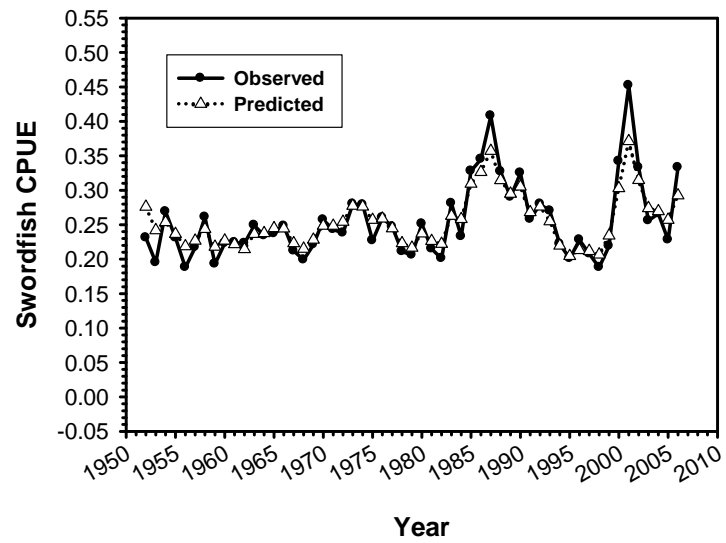
	Mean of Root Mean-Squared Error of Fit to Observed CPUE					
Stock Scenario	Japanese Longline	Taiwanese Longline	Hawaii Longline Shallow-Set 1	Hawaii Longline Shallow-Set 2	Hawaii Longline Deep-Set	California Gillnet
Single-Stock Scenario	0.126	0.338	0.264	0.195	0.627	0.964
Two-Stock Scenario Subarea 1	0.123	0.406	0.348	0.189	0.534	0.948
Two-Stock Scenario Subarea 2	0.267	0.339	-	-	-	-

Table 2. Mean estimates of intrinsic growth rate (R), carrying capacity (K), production model shape parameter (M), biomass to produce maximum sustainable yield (B_{MSY}), exploitation rate to produce maximum sustainable yield (H_{MSY}), maximum sustainable yield (MSY), exploitable biomass in 2006 (B_{2006}), probability that B_{2006} exceeds B_{MSY} , exploitation rate in 2006, and probability that H_{2006} exceeds H_{MSY} under the single-stock and two-stock scenarios.

Stock Scenario	Mean R	Mean K	Mean M	Mean B_{MSY}	Mean H_{MSY}	Mean MSY	Mean B_{2006}	Pr($B_{2006} > B_{MSY}$)	Mean H_{2006}	Pr($H_{2006} > H_{MSY}$)
Single-Stock Scenario	0.76	88.3	1.27	45.7	0.39	17.2	69.9	1.00	0.17	0.00
Two-Stock Scenario Subarea 1	0.63	96.2	1.05	47.9	0.29	13.5	55.5	0.82	0.19	0.01
Two-Stock Scenario Subarea 2	0.41	56.8	0.59	25.5	0.13	3.2	52.5	1.00	0.04	0.01

Figure 1.1. Time series of observed and predicted Japanese longline CPUE of swordfish along with standardized log-scale residuals of the model fit under the single-stock scenario during 1952-2006.

**Observed Japanese CPUE versus predicted CPUE
in the North Pacific Ocean by fishing year, 1952-2006**



**Standardized log-scale residuals of the production
model fit to Japanese CPUE in the North Pacific
Ocean by fishing year, 1952-2006**

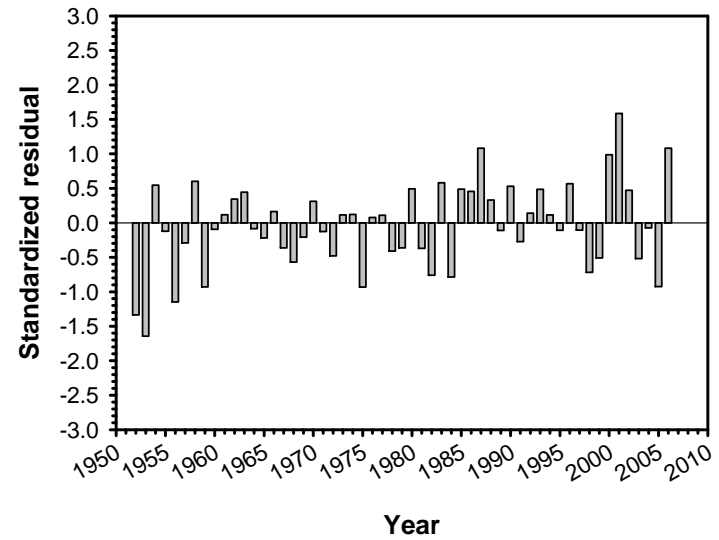
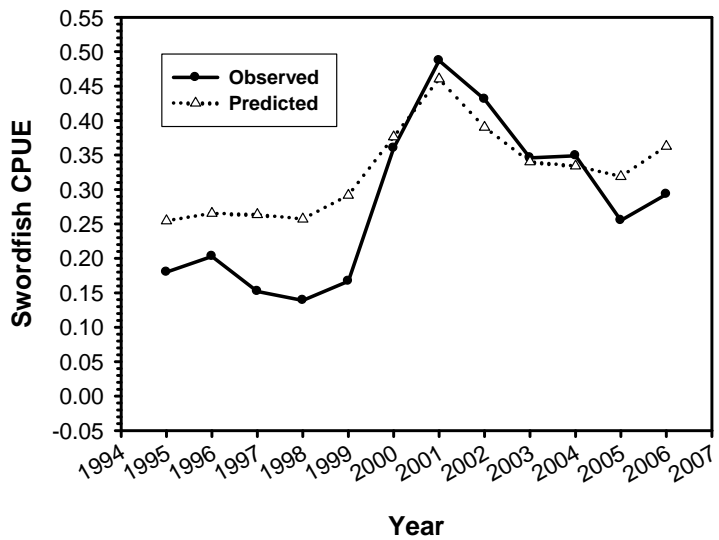


Figure 1.2. Time series of observed and predicted Taiwanese longline CPUE of swordfish along with standardized log-scale residuals of the model fit under the single-stock scenario during 1995-2006.

Observed Chinese-Taipei CPUE versus predicted CPUE in the North Pacific Ocean by fishing year, 1995-2006



Standardized log-scale residuals of the production model fit to Chinese-Taipei CPUE in the North Pacific Ocean by fishing year, 1995-2006

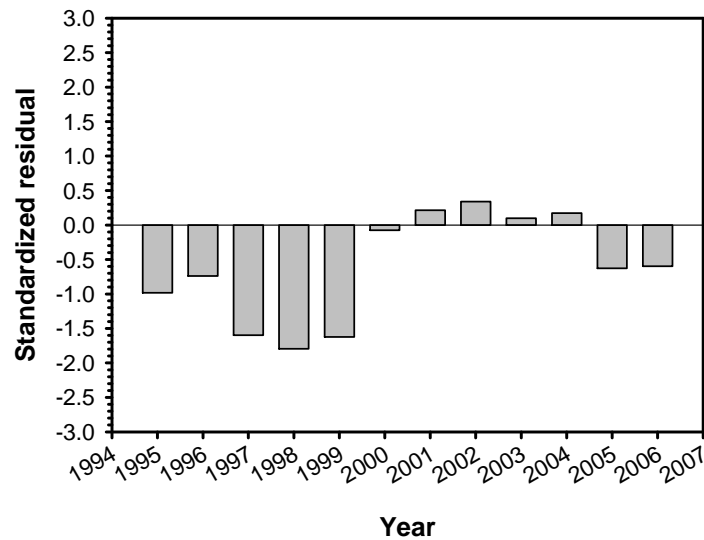
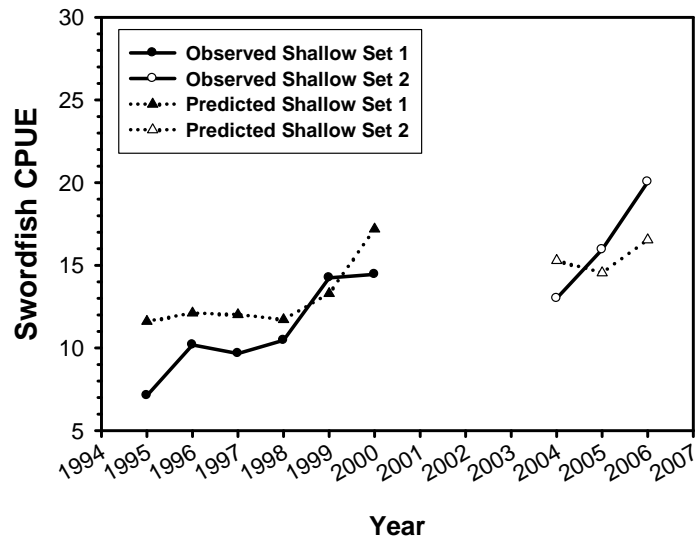


Figure 1.3. Time series of observed and predicted Hawaii shallow-set longline CPUE of swordfish along with standardized log-scale residuals of the model fit under the single-stock scenario during 1995-2000 and 2004-2006.

Observed Hawaii Shallow-Set CPUE versus predicted CPUE in the North Pacific Ocean by fishing year, 1995-2006



Standardized log-scale residuals of the production model fit to Hawaii Shallow-Set CPUE in the North Pacific Ocean by fishing year, 1995-2006

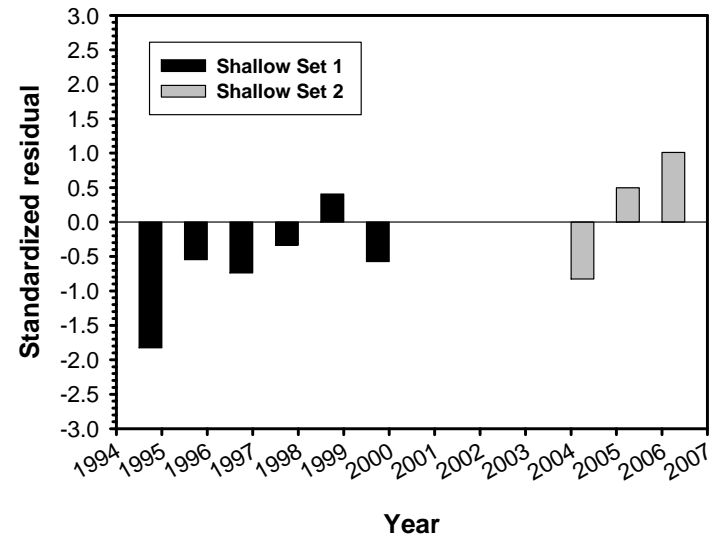
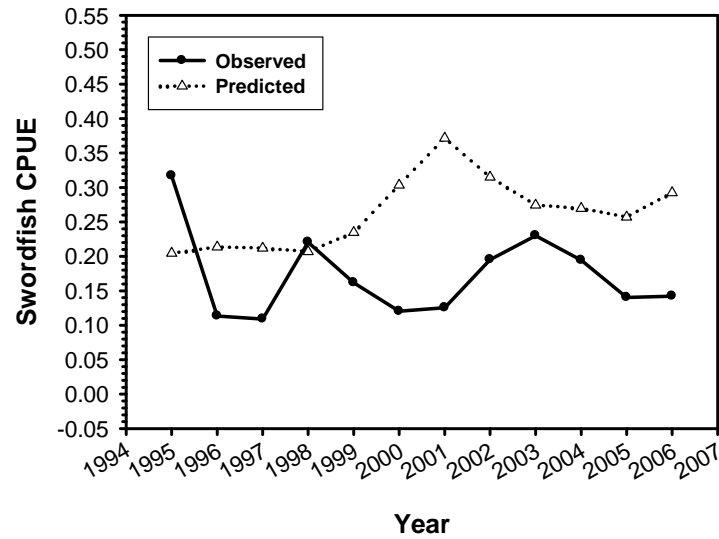


Figure 1.4. Time series of observed and predicted Hawaii deep-set longline CPUE of swordfish along with standardized log-scale residuals of the model fit under the single-stock scenario during 1995-2006.

Observed Hawaii Deep-Set CPUE versus predicted CPUE in the North Pacific Ocean by fishing year, 1952-2006



Standardized log-scale residuals of the production model fit to Hawaii Deep-Set CPUE in the North Pacific Ocean by fishing year, 1995-2006

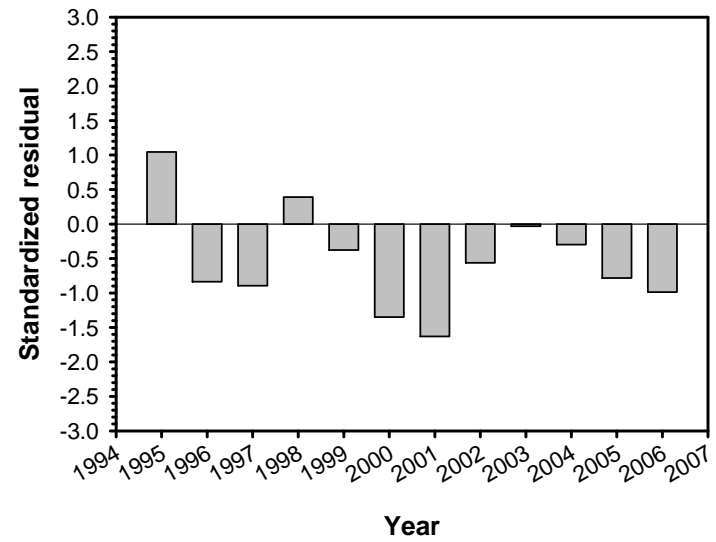
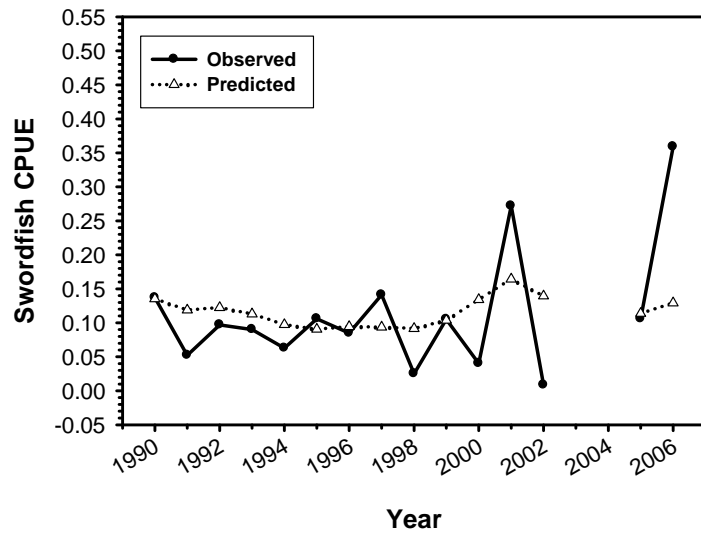


Figure 1.5. Time series of observed and predicted California gillnet CPUE of swordfish along with standardized log-scale residuals of the model fit under the single-stock scenario during 1990-2002 and 2005-2006.

Observed California Gillnet CPUE versus predicted CPUE in the North Pacific Ocean by fishing year, 1990-2006



Standardized log-scale residuals of the production model fit to California Gillnet CPUE in the North Pacific Ocean by fishing year, 1990-2006

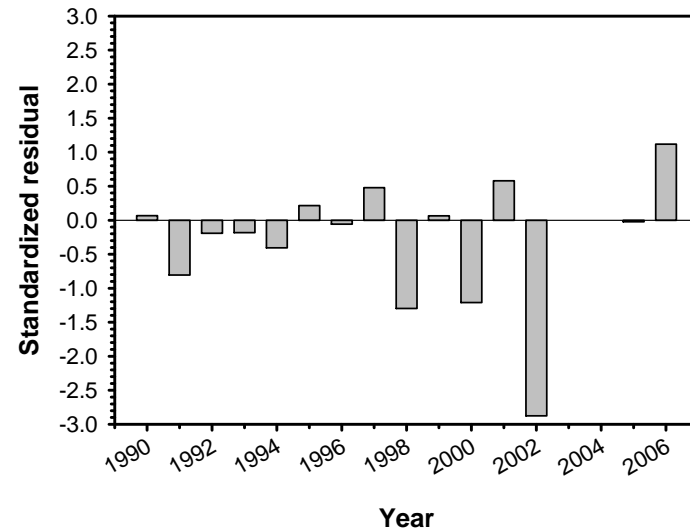
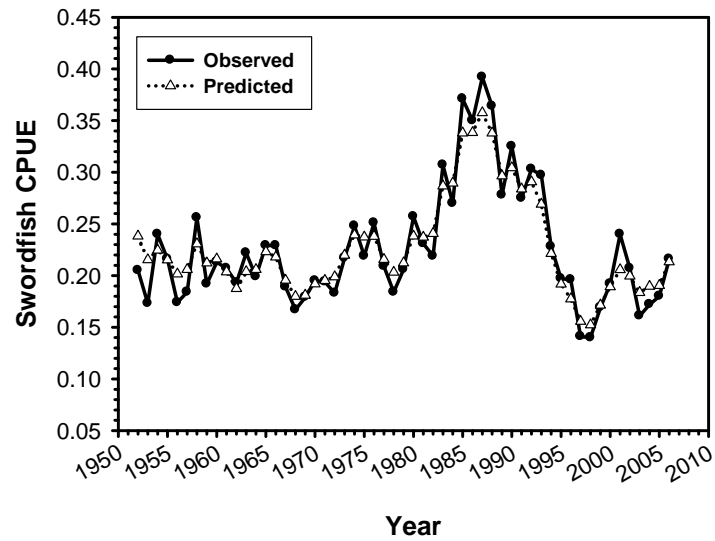


Figure 2.1. Time series of observed and predicted Japanese longline CPUE of swordfish in subarea 1 along with standardized log-scale residuals of the model fit under the two-stock scenario during 1952-2006.

**Observed Japanese CPUE versus predicted CPUE
in the North Pacific Sub-Area 1 by fishing year, 1952-2006**



**Standardized log-scale residuals of the production
model fit to Japanese CPUE in the North Pacific
Sub-Area 1 by fishing year, 1952-2006**

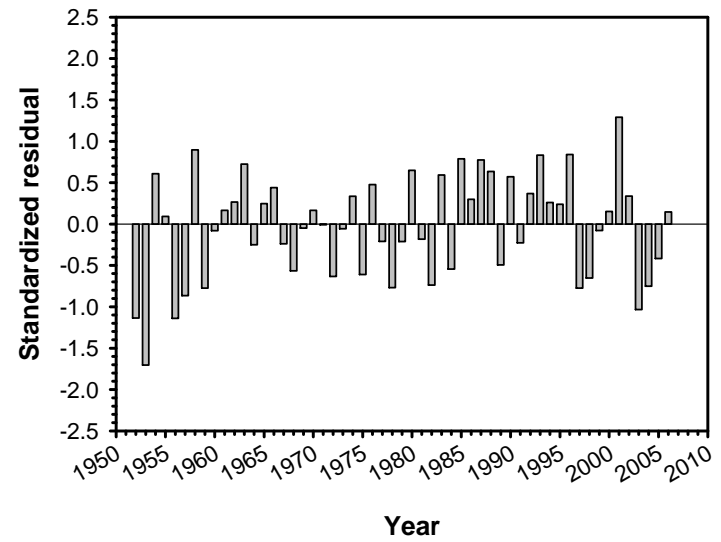
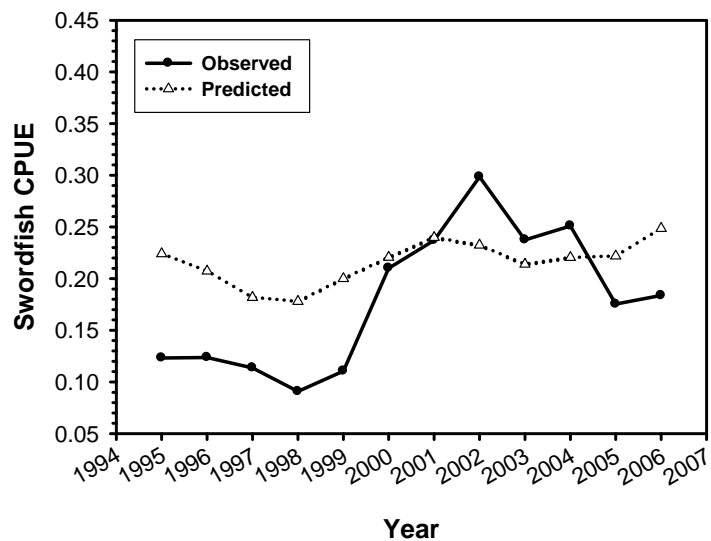


Figure 2.2. Time series of observed and predicted Taiwanese longline CPUE of swordfish in subarea 1 along with standardized log-scale residuals of the model fit under the two-stock scenario during 1995-2006.

Observed Taiwanese CPUE versus predicted CPUE in the North Pacific Sub-Area 1 by fishing year, 1995-2006



Standardized log-scale residuals of the production model fit to Chinese-Taipei CPUE in the North Pacific Sub-Area 1 by fishing year, 1995-2006

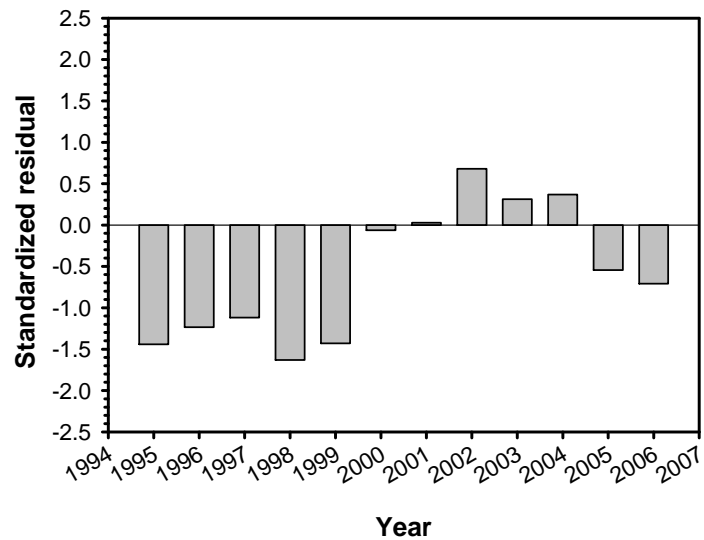
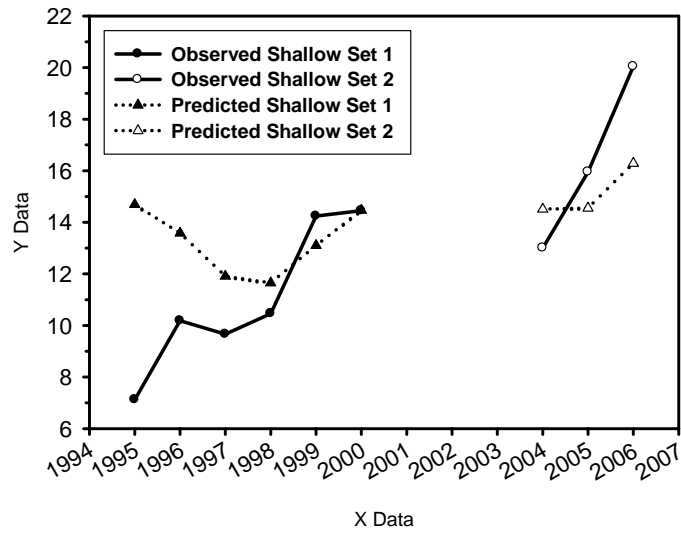


Figure 2.3. Time series of observed and predicted Hawaii shallow-set longline CPUE of swordfish in subarea 1 along with standardized log-scale residuals of the model fit under the two-stock scenario during 1995-2000 and 2004-2006.

Observed Hawaii Shallow-Set CPUE versus predicted CPUE in the North Pacific Sub-Area 1 by fishing year, 1995-2006



Standardized log-scale residuals of the production model fit to Hawaii Shallow-Set CPUE in the North Pacific Sub-Area 1 by fishing year, 1995-2006

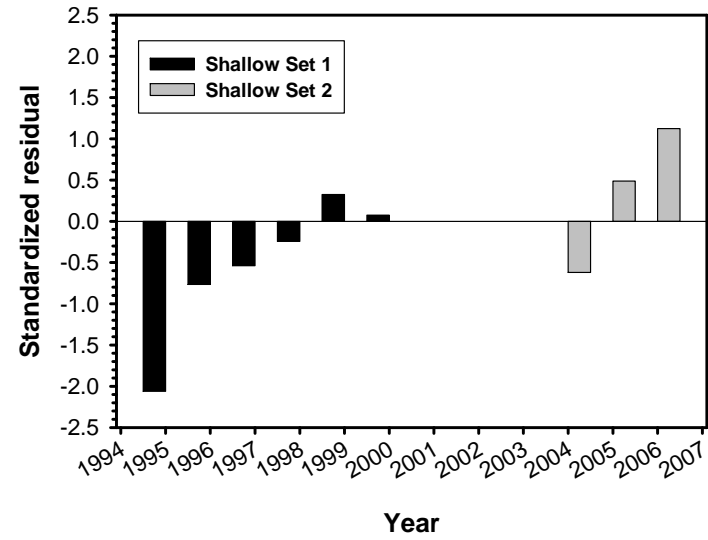
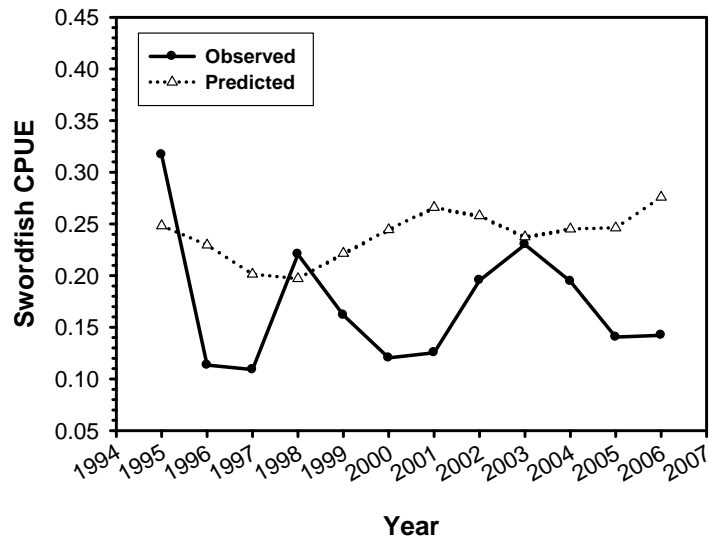


Figure 2.4. Time series of observed and predicted Hawaii deep-set longline CPUE of swordfish in subarea 1 along with standardized log-scale residuals of the model fit under the two-stock scenario during 1995-2006.

Observed Hawaii Deep-Set CPUE versus predicted CPUE in the North Pacific Sub-Area 1 by fishing year, 1995-2006



Standardized log-scale residuals of the production model fit to Hawaii Deep-Set CPUE in the North Pacific Sub-Area 1 by fishing year, 1995-2006

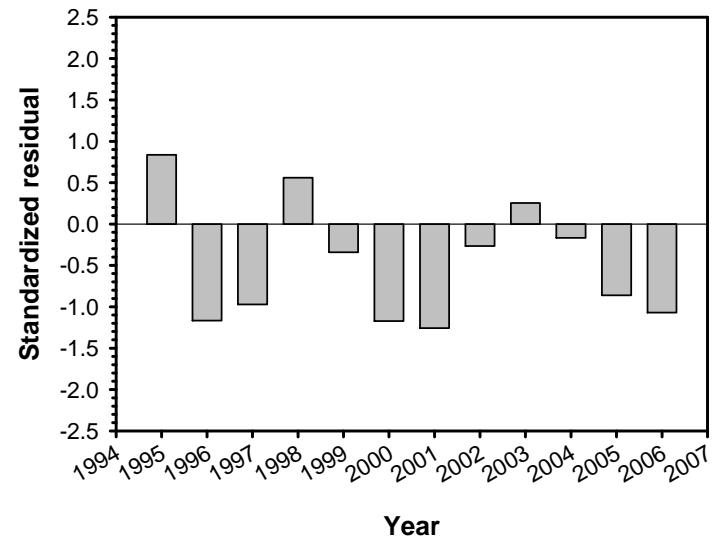
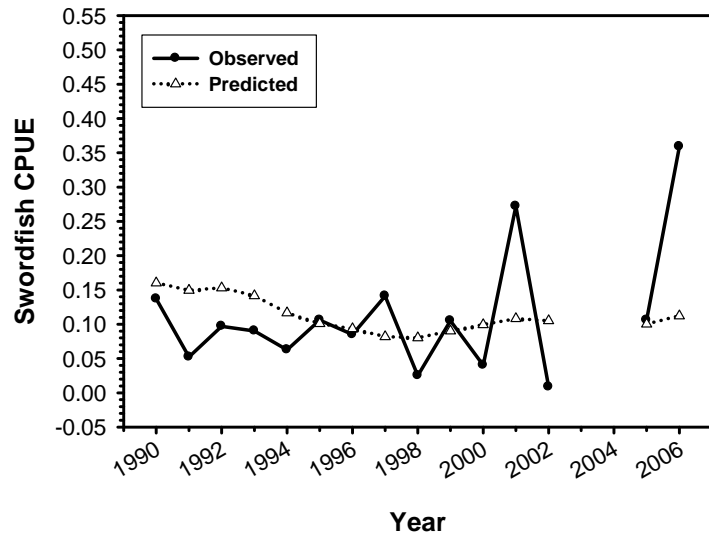


Figure 2.5. Time series of observed and predicted California gillnet CPUE of swordfish in subarea 1 along with standardized log-scale residuals of the model fit under the two-stock scenario during 1990-2002 and 2005-2006.

Observed California Gillnet CPUE versus predicted CPUE in the North Pacific Ocean by fishing year, 1990-2006



Standardized log-scale residuals of the production model fit to California Gillnet CPUE in the North Pacific Ocean by fishing year, 1990-2006

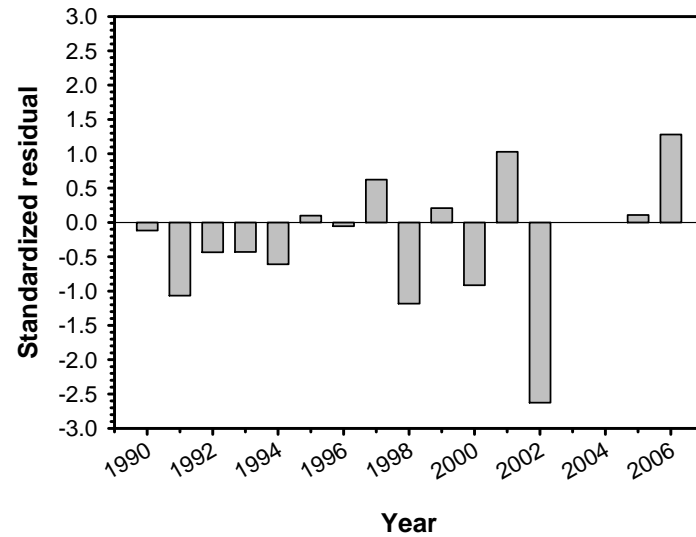
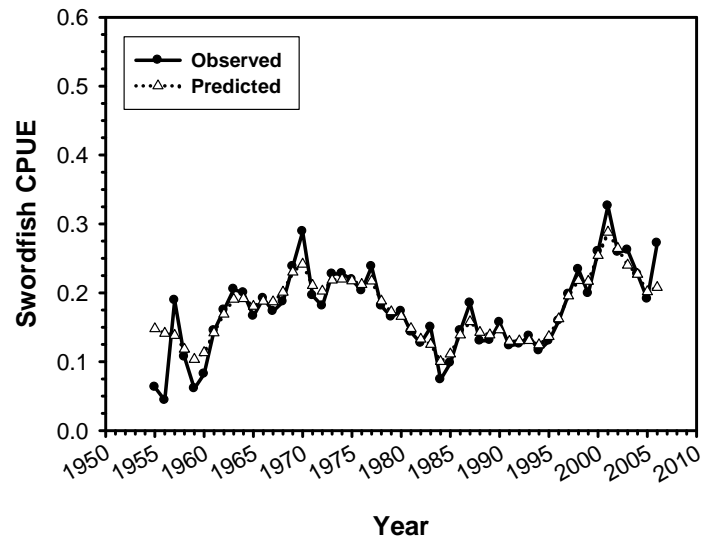


Figure 3.1. Time series of observed and predicted Japanese longline CPUE of swordfish in subarea 2 along with standardized log-scale residuals of the model fit under the two-stock scenario during 1955-2006.

**Observed Japanese CPUE versus predicted CPUE
in the North Pacific Sub-Area 2 by fishing year, 1955-2006**



**Standardized log-scale residuals of the production
model fit to Japanese CPUE in the North Pacific
Sub-Area 2 by fishing year, 1955-2006**

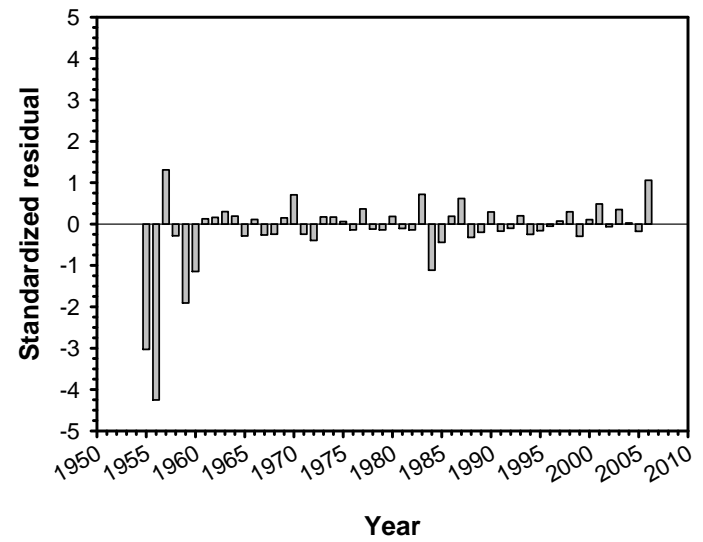
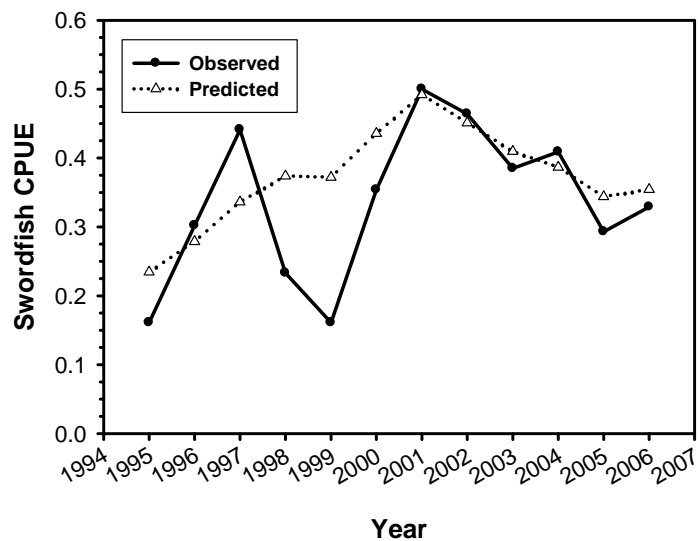


Figure 3.2. Time series of observed and predicted Taiwanese longline CPUE of swordfish in subarea 2 along with standardized log-scale residuals of the model fit under the two-stock scenario during 1995-2006.

Observed Chinese-Taipei CPUE versus predicted CPUE in the North Pacific Sub-Area 2 by fishing year, 1995-2006



Standardized log-scale residuals of the production model fit to Chinese-Taipei CPUE in the North Pacific Sub-Area 2 by fishing year, 1995-2006

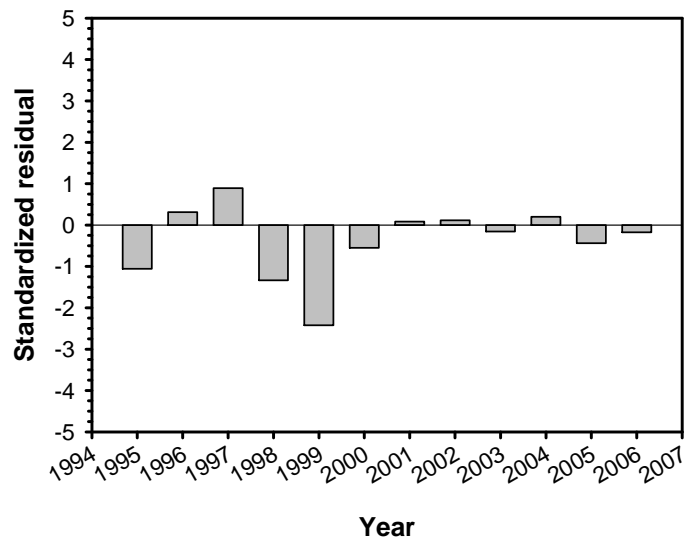


Figure 4.1. Trends in exploitable biomass and exploitation rate of North Pacific swordfish under the single-stock scenario, 1952-2006.

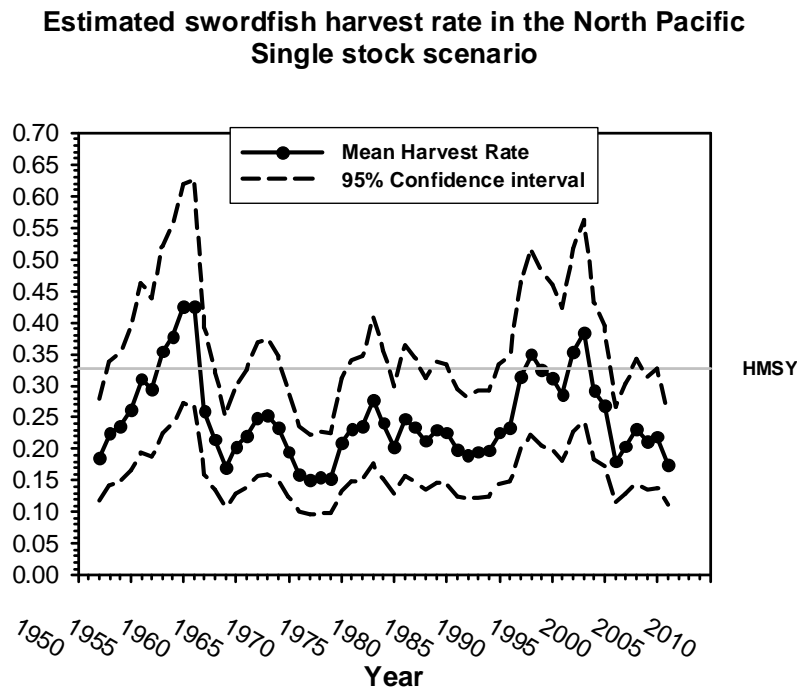
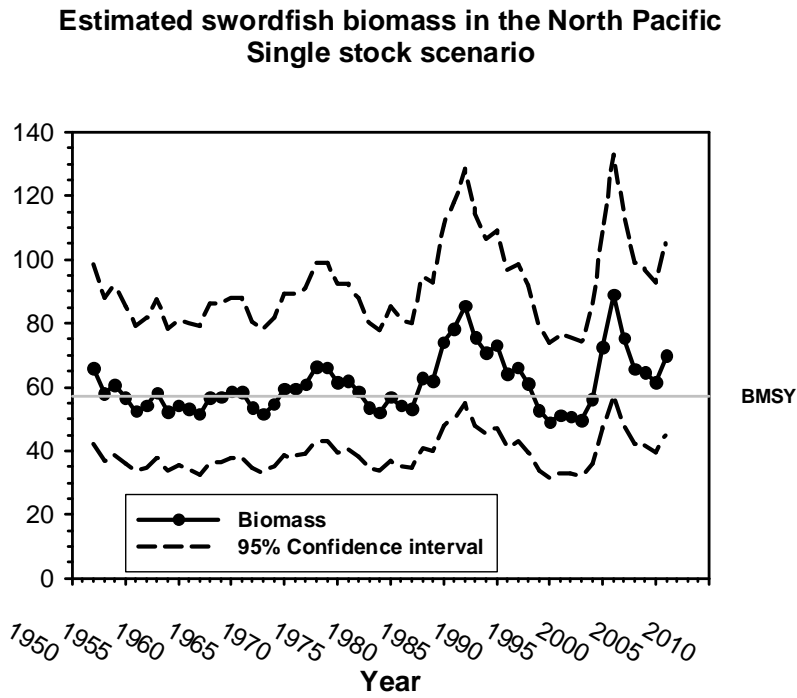
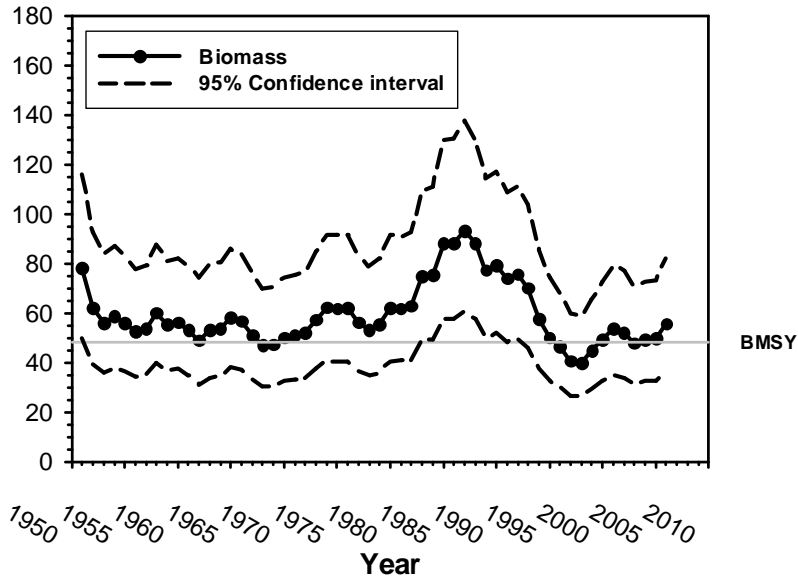


Figure 4.2. Trends in exploitable biomass and exploitation rate of North Pacific swordfish in subarea 1 under the two-stock scenario, 1951-2006.

**Estimated swordfish biomass in the North Pacific
Subarea 1**



**Estimated swordfish harvest rate in the North Pacific
Subarea 1**

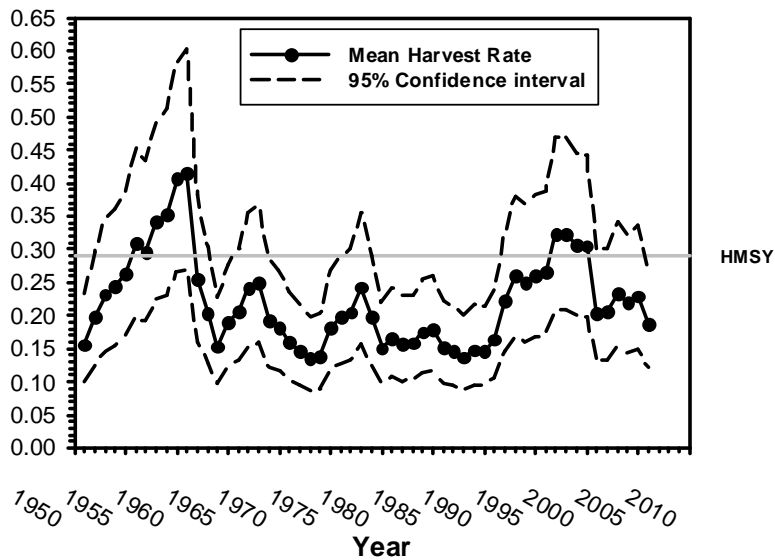


Figure 4.3. Trends in exploitable biomass and exploitation rate of North Pacific swordfish in subarea 2 under the two-stock scenario, 1951-2006.

